MEDIUM RESOLUTION STUDIES OF EXTREME ULTRAVIOLET EMISSION FROM COBY ELECTRON IMPACT

lsik Kanik, Geoffrey K. James and Joseph M. Ajello

Jet Propulsion Laboratory, California Institute of Technology, Pasadena, CA 91109

SECOND REVISION

SUBMITTED TO:

Phys. Rev. A

September 29, 1994

ABSTRACT

We report medium resolution *(0.025* nm FWHM) electron-impact induced emission spectra of CO for 20, 100 and 200 eV impact energies. The mission spectra correspond to the extreme ultraviolet (EUV) transitions from the $B\,^1\Sigma^+(0)$, $C\,^1\Sigma^+(0)$ and $E\,^1\Pi(0)$ vibronic states to the $X\,^1\Sigma^+(0)$ ground state. The present measurements are carried out at 20 times higher spectral resolution (to seperate the many blended components) compared to our previous measurements which were at a Spectral resolution of 0.5 nm FWHM. The emission cross sections corresponding to the $B\,^1\Sigma^+(0)\rightarrow X\,^1\Sigma^+(0)$, $C\,^1\Sigma^+(0)\rightarrow X\,^1\Sigma^+(0)$ and $E\,^1\Pi(0)\rightarrow X\,^1\Sigma^+(0)$ transitions were measured. in addition, excitation functions (O-1 keV) extending well into the Born region have been measured for the strong transitions ($B\,^1\Sigma^+(0)\rightarrow X\,^1\Sigma^+(0)$, $C\,^1\Sigma^+(0)\rightarrow X\,^1\Sigma^+(0)$) and oscillator strengths have been determined using a modified Born approximation analytic fit to the measured excitation function.

INTRODUCTION

Carbon monoxide is the most abundant interstellar molecule after 112 and its isotopic variants [1] and is an important constituent in the atmosphere of Venus [2]. Theoretical descriptions of the abundance, excitation and destruction mechanisms of CO arc limited due to the lack of quantitative spectroscopic data for (X) in the vacuum ultraviolet (VUV) region [3]. A better understanding of the destruction of CO is necessary for studies of airglow emission from planetary atmospheres, as well as for studies of comets and for models of the chemistry of the interstellar medium [2]. Photochemical models of interstellar clouds have been described in detail by numerous investigators [4-8]. The main destruction mechanism for CO in the interstellar regions is considered to be photodissociation. The relative abundance of CO (relative to 112) in the interstellar region has not been well understood theoretical 1 y. The rate at which the CO molecule is photodissociated by UV starlight is one of the major theoretical uncertainties [1]. This rate governs the C/CO ratio, the abundance of CO and its growth with depth in diffuse interstellar clouds and the outer parts of thick molecular clouds [1]. Reviews of photodissociation processes of astrophysical molecules which emphasize the need for improved data for CO were compiled by van Dishoeck [9, 10]. Most recently Morton and Noreau [11] have compiled wavenumbers, wavelengths and oscillator strengths for about 1500 electronic transitions in the CO molecule and compared the compiled data with existing UV observations.

Photodissociation of CO occurs in the wavelength range $91.2 < \lambda < 111.8$ nm [1]. Numerous experimental studies of the electronic states of CO lying above the dissociation limit have been performed in recent years [3, 12-2A]. Photodissociation of a molecule can take place either directly by continuous absorption into the repulsive part of an excited electronic state, or indirectly by discrete line absorption into predissociating states [9]. Laboratory experiments have revealed no significant continuous absorption into the repulsive part of an excited electronic state al wavelengths greater than 91.2 nm [3, 14, 15, 17]. Quantum mechanical calculations of the electronic structure of CO by Cooper and Kirby [25] supported this conclusion. It was, therefore, concluded that the dissociation of CO must take place predominantly through predissociation of bound states and not directly through continuum states [1]. In order to fully

understand the abundance, excitation and dissociation mechanisms of CO in the interstellar medium, high resolution spectroscopic studies of C() in the energy range *10.7 -13.6* CV arc required.

In this paper, wc report, as a continuation of our previous work *[20],* the electron-impact induced emission spectra of CO corresponding 10 the 1 :UV transitions from the $B\,^1\Sigma^+$, $C\,^1\Sigma^+$ and $E\,^1\Pi$ 1 states to the $X\,^1\Sigma^+$ ground state for 20, 100 and 200 CV electron impact energies. in order to separate the many blended spectral bands, the present measurements were carried out at 2.0 times higher spectral resolution (FWHM=0.025 mu) than our previous measurements. Emission cross sections corresponding to the $B\,^1\Sigma^+(0) \rightarrow X\,^1\Sigma^+(0)$ $C\,^1\Sigma^+(0) \rightarrow X\,^1\Sigma^+(0)$ and $E\,^1\Pi(0) \rightarrow X\,^1\Sigma^+(0)$ transitions were measured. In addition, excitation functions (O-1 kcV) extending wc]] into the Bor u region have been measured for the resonance transitions ($B\,^1\Sigma^+(0) \rightarrow X\,^1\Sigma^+(0)$, $C\,^1\Sigma^+(0) \rightarrow X\,^1\Sigma^+(0)$) allowing the oscillator strengths to be determined using a modified Born approximation analytic fit to the shape of the measured excitation function [26, 2.7].

EXPERIMENTAL APPARATUS

The experimental apparatus, calibrat ion procedure aud cross section measurement technique have been described in our recent publications [28, ?9]. In brief, the medium resolution 1 .O-meter spectrometer system was used in the present measurements. It consists of an electron -impac.t collision chamber in tandem with a UV spectrometer. The spectrometer has a resolution capability of 0.025 nm on repeated aud single spectral scans. The resolution capability was verified by scanning the Ar 104.8 nm resonance line. With equal entrance and exit slits the instrument response function was triangular. UV emission spectra of CO were measured by crossing a magnetically collimated beam of electrons with a beam of CO gas formed by a capillary array. 1 :mitted photons, corresponding to radiative decay of collisionally excited states of CO were detected by the U JV spectrometer equipped with a chaneltron detector. The resulting emission spectra, measured at 20, 100 aud 200 CV incident electron beam energies were calibrated for relative sensitivity as a function of wavelength according to the procedures dcscribcd by Ajello et al. [30]. in order 10 determine the absolute value of the emission cross section corresponding to each measured feature, one additional procedure (normalization) must be applied. The absolute cross

section of the spectral feature at 83.38 nm, at 200 eV electron impact energy, was chosen to normalize the relative intensities of the $B^1\Sigma^+$ (0), C $^1\Sigma^+$(0) and E^{1}1 l(O) vibronic states of CO. The OII (83.38 nm) fluorescence signal produced by dissociative ionization of CO at 200 CV impact energy was compared with the fluorescence signal from the CO C ’22(0)- ›X *X$^+$(0) emission band at 108.79 nm at 200 CV impact energy under the identical gun conditions. A background gas pressure about 1 x 10-5 Torr was used to avoid self absorption effect on the $C^1\Sigma^+$ (0,0) band as discussed below. A well-cs(ablisbed absolute emission cross section value of 1.8 ± 0.39 x 10^{-19} cm^2 for OII (83.38 nm)[20], at 200 cV, was used to normalize the signal strength of the CO $C^1\Sigma^+$ (0,0) hand, at 200 cV, to an absolute emission cross section value of 58.9 ± 14.7 x 10^{-19} cm^2.

The background gas pressure for the present determination of CO emission cross sections was carefully chosen to ensure optically tbiu conditions and to avoid self-absorption effects, particularly for the $C^1\Sigma^+$ (0,0) band at 108.79 nm. The operat ing pressure must result in an optical depth at line center of less than 0.1 for the optical path involved. Below this pressure the measured cross section will be independent of pressure. The following approach has been used to determine the maximum background gas pressure that can be used and still maintain optical I y thin conditions. The relative intensities of the C $^1\Sigma^+$ (0,0) band at 108.79 nm and the 011 $g\,^4S^0$- ^{4}1’ multiplet at 83.38 nm have been measured as a function of pressure over the range 8 x 10^{-8} to 8 x 10^{-4} Torr. The OII line is not expected to exhibit any optical depth effects in this pressure range and acts as a normalization feature. The intensity ratio of these features is shown in Fig.1 and is approximately constant up (o a background gas pressure of 2 x 10^{-5} Torr when it begins to decrease, indicating the effect of self-absorption at 108.79 nm.

No corrections for polarization of the radiation were made. Polarization of the radiation was considered to be small where many rotational states contribute to a vibrational band for an excited molecule.

EXPERIMENTAL RESULTS AND I) ISCUSSION

Medium-rcsolotion, electron impact emission spectra of CO in the EUV region, at 20, 100 and 200 cV, arc shown in Figs. 2, 3 and 4 respectively. These spectra were obtained under optically thin

conditions, at a spectral resolution of 0.025 nm (FWHM), and calibrated for wavelength. The background gas pressure was 1 x 10-5 Torr. The spectral features arc identified in the figures. The spectral region from 107.4 to 109.2 nm includes the direct EUV transitions from the E $^1\Pi$(O) and C $^1\Sigma^+$(0) excited vibronic states of (X). At the present resolution, the observed 1:$^1\Pi$(0) and C $^1\Sigma^+$ (0) features correspond exclusively to molecular transitions in CO. The spectral region from 114,8 to 115.4 nm contains the EUV transition from the B $^1\Sigma^+$(0) excited state of CO, which is blended with an atomic component (0111)-11)0 at 115.2 nm) at 100 and 200 eV electron impact energies. (Figs. 3 and 4). At 20 cV, an energy below the threshold for dissociative excitation of atomic multiplets, the B $^1\Sigma^+$ feature corresponds purely to molecular transitions in CO. '1'able 1 lists the candidate identifications of each feature observed at this spectral resolution together with the measured absolute emission cross sections at 20, 100 and 200 CV electron impact energies. The root sum square uncertainty in the absolute cross sections given in this work was estimated to be 2S % based on the uncertainties in the OII(83.3 nm) cross section, relative calibration and signal statistics [28].

The strongest feature observed in the 100 and 2(K) CV emission spectra of CO corresponds to the (' $^1\Sigma^+ \rightarrow$ X $^1\Sigma^+$ (0,0) resonance band. This feature contains approximately 98% of the observed EUV mission between the C $^1\Sigma^+$ state and the X $^1\Sigma^+$ stale [20]. This is supported by consideration of unperturbed RKR Fran ck-Condon factors calculated for the C- ›X system. I etzelter et al. reported the branching ratio loss to be 7% via the C- ›A mission channel [17]. Excitation functions measured in the ranges 0-250 CV and O-1.0 keV arc shown in Fig. 5 and Fig. 6 respectively. The excitation function shapes arc typical of a dipole allowed transition. The excitation function for CO C $^1\Sigma^+ \rightarrow$ X $^1\Sigma^+$ (0,0) resonance band al 108.79 nJn, from O m 25(J CV (Fig. 5), was used 10 determine the 2(KJ to 20 CV and 200 to 100 CV emission cross section ratios. These ratios were needed to obtain the absolute emission cross sections for the CO C $^1\Sigma^+$ (0) -> X $^1\Sigma^+$ (()) band at ?0 and 100 CV electron impact energies at 0.025 nm (FWHM) spectral resolution.

The strongest feature observed in our 20 CV spectrum is the B $^1\Sigma^+$ -> X $^1\Sigma^+$ (0,0) band, Based on our previous paper [20], the B $^1\Sigma^+$› X $^1\Sigma^+$ (0,0) band represents 96% of the observed EUV emission from the B slate of (X). The B stale decays only by Iwo radiative channels: through B- ›X transitions in

the UV and through B-›A transitions in the visible spectral region. 1 etzelter et al. reported the fluorescence yield of the B-›A transition (i.e. branching ratio loss) as 40% [17]. As shown in Fig. 7, $B\,^1\Sigma^+ \rightarrow X\,^1\Sigma^+$ (0,0) band exhibits a striking anomaly in the energy dependence of its emission cross section. in our earlier publication [20], wc argued that this may be attributed either to an electron exhange process or to a near threshold resonance of the 01 multiplet which blended with the $B^1\Sigma^+$ (0,0) feature. The higher spectral resolution (0.0'2S nm)-excitation function measurement of the $B^1\Sigma^+$ (0) vibronic state indicated that spin exchange plays a large part in the excitation of the v'=0 level of the $B^1\Sigma^+$ state (since the Ol multiplet was resolved and excluded from this measurement). This is also supported by differential cross section measurements for the electron-impact excitation of the $D\,^1\Sigma^+$ slate at 20 CV [23]. '1'heir measurements showed no strong forward peaking but fairly isotropic angular distribution. It should be pointed out that even though the B state is designated as a singlet stale, the very sharp peak in the excitation function of the $B^1\Sigma^+$(0) state (Fig. 7), at low electron impact energies, should arise from spin exchange from a significant triplet admixture. The singlet character of this state dominates at higher energies in the excitation function.

The] ;1I 1-> $X\,^1\Sigma^+$ system was observed in our spectra by the apparance of the (0,0) resonance band. No excitation function measurement for the $E\,^1I\,1$ (0) –› $X\,^1\Sigma^+$ (0) transition was made since the emission from this band is found to be very weak. No other transitions of the 1 :-›X system were observed. RKR Franck-Condon factor calculations, on the other hand, indicate that about 95% of the EUV emission from this state to the ground state occurs via the (0,0) transition [20].

Oscillator Strengths

Previous experimental and theoretical determinations of oscillator strengths $f_{v'v''}$ from v"=0 of the $X\,^1\Sigma^+$ ground state of CO to different v' levels of the $B\,^1\Sigma^+$ and $C\,^1\Sigma^+$ states have been summarized by Kirby and Cooper [2]. This summary has been updated to include the work of Chan et at. [22] and is shown, together with present results in '1'able 11.

We obtain the oscillator strengths for the $C\,^1\Sigma^+$ (v'= O) -> $X\,^1\Sigma^+$ (v"= O) and $D\,^1\Sigma^+$ (v'= O) -> $X\,^1\Sigma^+$ (v"= O) transitions by analyzing the energy dependence of the measured excitation functions (from O

m I keV) corresponding to those transitions. The excitation functions for the C $^1\Sigma^+$ (v'= O) -> X $^1\Sigma^+$ (v"= ()) and B $^1\Sigma^+$ (v' = O) → X $^1\Sigma^+$ (v" = O) transitions (figures 6 and 7 respectively) arc put cm an absolute scale by normalizing them to the presently measured 200 CV emission cross sections for the C $^1\Sigma^+$ (v'=0) › X $^1\Sigma^+$ (v"=0) and B $^1\Sigma^+$ (v'=O)- › X $^1\Sigma^+$ (v"=0) transitions, respectively. The emission cross sections for the B -X (0,0) and C-X (0,0) vibronic states, given in Table 1, were corrected for the branching ratio losses to a lower excited slate (A $^1\Pi$) based on the 1 etzelter et al. [17] data. Tbc correction is 40% for the B-X(0,0) state and 7% for the C-X (0,0) state. Cascade contributions from the 1; $^1\Pi$ state to the D-X (0,0) and C-X (0,0) is negligible [20].

Collision strength data (cross section x electron impact energy) for the resonance bands of CO (C $^1\Sigma^+$ and B $^1\Sigma^+$) were fitted using the following analytical form for collision strength:

$$\Omega_{v'v''}(X_{v'v''}) = C_o \cdot (1-1/X_{v'v''}) \cdot (X_{v'v''}^{-2}) + \sum_{k=1}^{4} C_k \cdot (X_{v'v''} - 1) \cdot \exp(-k \cdot C_8 \cdot X_{v'v''}) + C_5 + C_6 / X_{v'v''} + C_7 \cdot \ln(X_{v'v''}) \quad (1)$$

where $\Omega_{v'v''}(X_{v'v''})$ is the collision strength, $X_{v'v''}$ is the electron impact energy in threshold units, and C_k arc constants of the function $\Omega_{v'v''}(X_{v'v''})$ [26, 27]. The constant C_o represents the contribution of electron exchange, C_1-C_4 represent configuration mixing, C_5-C_6 represent polarization effects, C_7 is the Rorn term and C_8 is a constant in the mixing terms. Table 111 gives the constants of eqn. 1 for the CO B $^1\Sigma^+$ (v'= 0)- › X $^1\Sigma^+$ (v"=0) and C $^1\Sigma^+$ (v'= 0)- › X $^1\Sigma^+$ (v"=0) transition s.The excitation cross section is given by the equation

$$\sigma_{v'v''}(X_{v'v''}) = \Omega_{v'v''}(X_{v'v''}) \cdot (E_{v'v''} \cdot X_{v'v''})^{-1}, \quad (2)$$

where $\sigma_{v'v''}(X_{v'v''})$ is the cross section in atomic units, and $E_{v'v''}$ is the transition energy in Rydberg units. At the high energy limit the collision strength has the following form:

$$\Omega_{v'v''}(X_{v'v''}) \approx C_5 + C_7 \cdot \ln(X_{v'v''}), X_{v'v''} >> 1 \quad (3)$$

in the Bethe Approximation [27,31], the collision strength is given by

$$\Omega_{v'v''}(X_{v'v''}) = \omega_{v''}\left(\frac{8ma_0^2}{\hbar^2 E}\right)\frac{f_{v'v''}}{\cdot\,{}_{v'v''}}(\mathrm{In}\ X_{v'v''} - \mathrm{i}\ 4C_{v'v''}E_{v'v''}) \qquad (4)$$

where $\omega_{v''}$ is the lower state degeneracy, $C_{v'v''}$ is a constant, related to the angular distribution of the scattered electrons, $f_{v'v''}$ is the oscillator strength, a_o is the Bohr radius, m is electron mass, and $\hbar$ is the Planck's constant. Comparison of equations (3) and (4) gives us C_7, one of the constants in the fitting function, which can be related to the optical oscillator strength at the high energy limit. That is,

$$C_7 = \omega_{v''}\left(\frac{8ma_0^2}{\hbar^2}\right)\frac{f_{v'v''}}{E_{v'v''}} \qquad (5)$$

As seen in Eqn. (5), we can determine the optical oscillator strength. For the CO C $^1\Sigma^+$ (0)→ X $^1\Sigma^+$ (0) and B $^1\Sigma^+$ (0)- › X $^1\Sigma^+$ (0) transitions the optical oscillator strengths were found to be 15.4 ± 4.1 x 10^{-2} and 1,15 ± 0.3 x 10^{-2} respectively. The experimental excitation function and the fitting function for the CO C $^1\Sigma^+$ (0)- › X $^1\Sigma^+$ (0) and B $^1\Sigma^+$ (0)- › X $^1\Sigma^+$ (0) transitions arc shown in Fig. 8 and Fig. 9, respectively.

The errors asscoiated with the oscillator strengths arc estimated as follows: (a) 25% error from our the cross-section measurements and (b) 5% error from the fitting procedure. In addition, it should be pointed out that the presence of the low energy secondary electrons in the electron beam could alter the shape of an excitation function in the high energy region and hence potentially give an increase to the measured value of C_7 and hence the optical oscillator strength. Our measurements [32] showed that this effect could give us an additional error up to 10% in the oscillator strength. Thus the overall error (square root of the sum of the squares of the contributing errors) in the oscillator strengths is estimated to be about 27%.

'1'here arc many reported experimental measurements of the oscillator strength of the B $^1\Sigma^+$ and C $^1\Sigma^+$ states. Large variations have been found among these values. For the B $^1\Sigma^+$ (0) -> X $^1\Sigma^+$ (0) transition, comparison of the oscillator' strengths gives a fair agreement between the present finding and the results of Aarts and deHeer [1?], 1 .assettre and Skerbele [13] and Chan et al. [22]. The present result is about 30% lower than that of Aarts and deHeer [1?] and 33% lower than that of Lassettre and Skerbele [13]. The present measurement is, however, about 30% larger than the most recent result of Chan et al.

[22]. The discrepancy between the present measurement and the results of other investigators [2, 15, *17] is* found to be quite large. The other results arc 2.5 to 5.5 times smaller than the present result.

For the C $^1\Sigma^+$(0) $\rightarrow$ X ^{1}X+(0) transition, comparison of the oscillator strengths gives an excellent agreement between the present result and those of Aarts and dc Heer [12] (4 % higher than ours) and Lassettre and Skerbele [13] (about 6% higher than ours). The theoretical result of Kirby and Cooper [12] is about 23% lower than ours. The value of Lee and Guest [15] is smaller than ours by an order of magnitude. Our value is about 2.5 times larger than the measurement of I x.welter cl al. [17]. 1 lowever, our study shows that the C$^1\Sigma^+$ band is subject to pressure saturation effect. Since pressure effects increase with increasing oscillator strength, the effect of self-absorption of radiation in the C state will be much larger than for the B state. Therefore, the values of the oscillator strengths reported by I ee and Guest [15] and I etzelter c(al. [17] for the C$^1\Sigma^+$ - › X $^1\Sigma^+$ transition may well be affected by pressure saturation effects. The most recent result of Chan et al. [22] is in fairly good agreement with the present result (the disagreement is about 23%).

SUMMARY ANI) CONCLUSION

We have measured the electron impact induced emission spectra of CO corresponding to the EUV transitions of the B$^1\Sigma^+$, C$^1\Sigma^+$ and E$^1\Pi$ states to the X $^1\Sigma^+$ ground state for 20, 100 and 200 CV electron impact energies. The present measurements were. carried out at a spectral resolution of 0.025 nm (l'WJIM). Excitation function measurements from 0 to 1.0 keV fOr two resonance transitions (C$^1\Sigma^+$(0)–› X $^1\Sigma^+$(0) and D $^1\Sigma^+$(O)- › X $^1\Sigma^+$(0)) were performed. The corresponding oscillator strengths were determined using a modified Born approximation analytic fit to the shape Of the measured excitation function [26, 27]. For the B$^1\Sigma^+$(0)--> X $^1\Sigma^+$(0) transit ion, comparison of the oscillator strengths gives a fair agreement between the present finding and the results of Aarts and deHeer [12], Lassettre and Skerbele [13] and Chan et al. [22]. The disagreement between the present and other results is, however, quite large, as seen in '1'able II. For the C$^1\Sigma^+$ - › X $^1\Sigma^+$ process, comparison of the oscillator strengths gives an excellent agreement with the experimental values of Aarts and dc 1 leer [12], Lassettre and Skerbele [13]. The experimental value of Chan et al. [??] and the theoretical value of Kirby and Cooper

[2] arc in fairly good agreement with our result. Large discrepancies exist between the other reported sets and the present result.

Serious discrepancies exist among the limited measurements of cross sections and oscillator strengths reported for CO. There is a definite need for further measurements 10 improve on the present situation. Further investigations of this type, at room temperature and at low temperature regime, arc needed. The importance of low temperature measurements to learn more details about the molecular clouds was pointed out by Dishoeck and Black [10].

The scope of this paper is limited to the measurement of the emission cross sections and oscillator strengths of the direct EUV transitions m the ground slate. 1 lowever, the importance of accurate determination of the predissociation rates for the excited states of CO was strongly emphasized by several investigators [1, 3, 19]. The predissociation rates for the low rotational levels of both the $E^1\Pi$ (0)--> $X\ ^1\Sigma^+$ (0) and $1\ ^1\Pi$ 1 (1)-- › X $'X^+$(0) bands arc, especially, very important to understand the isotope-sclcctivc photodissociation of CO [1]. The emission cross sections can be used to estimate the predissociation yields by comparison with the corresponding electron impact excitation cross sections obtained from electron energy-loss measurements provided any cascading components to and from (i.e. branching loss) the states in question arc taken into account. This type of approach, however, is not very meaningful way to determine small predissociation yield (typically 20% or smaller) of a state if the predissociation yield (%) lies within the combined percent error limit (typically about 25%) for the emission and the excitation cross sections. Instead, a high resolution study of the properties of CO rotational structure at a variety of temperatures (20-300 K), employing the Perturbed Thermal Mode.1 [33] fit to the data, is a more meaningful and sensitive probe for weak predissociation. This approach has been used for the determination of predissociation yields of the C4' $^1\Sigma^+$ (0)- › X $^1\Sigma^+$ (0) state of N2 [32]. 1 aboratory measurements of high spectral resolution (up to 0.0015 nm), optically thin UV emission spectra of CO, at a variety of temperatures (20-300 K), arc in progress to determine J-level dependent predissociation rate.s.

ACKNOWLEDGMENTS

This work was carried out at the Jet Propulsion Laboratory, California Institute of Technology, and was supported by the National Aeronautics and Space Administration, the Aeronomy program of the National Science Foundation and by the Air Force office of Scientific Research. The authors benefitted from discussion with Sandor Trajmar and Donald Shemansky.

References

[1] E. F. van Dishoeck and J. H. Black, *Astrophys. J. 334,771* (1988).

[2] K. Kirby and D. L. Cooper, J. Chem. Phys. 90,4895 (1989).

[3] G. Stark, K. Yoshino, P. L. Smith, K. Ito and W. H. Parkinson, Astrophys. J. 369,574 (1991).

[4] J. H. Black and A. Dalgarno, Ap. J. Suppl. 34,405 (1977).

[5] E. F. van Dishoeck and J. H. Black, Astrophys. J. Suppl. 62, 109 (1 986).

[6] E. F. van Dishoeck and J. H. Black, *Physical Processes in Interstellar Clouds*, ed. G. E. Morfill and M. Scholer (Reidel, New York, 1987), p.241.

[7] E. F. van Dishoeck and J. H. Black, *Rate Coefficients in Astrochemistry*, ed. T. J. Millar and D. A. Williams (Kluwer Academic, Deventer, 1988), p.209.

[8] E. F. van Dishoeck, *Highlights of Astronomy*, ed. D. McNally (Reidel, Dordrecht, 1989), p.323.

[9] E. F. van Dishoeck, *Astrochemistry*, ed. M.S. Vardya and S. P. Tarafdar (1987), p.51.

[10] E. F. van Dishoeck, *Rate Coefficients in Astrochemistry*, ed. T. J. Millar and D. A. Williams (Kluwer Academic, Deventer, 1988), p.49.

[11] D. C. Morton and L. Noreau (private communication, 1994).

[12] J. F. M. Aarts and F. J. de Heer, J. Chem. Phys. **52**, 5354 (1970).

[13] E. N. Lassettre and A. Skerbele, J. Chem. Phys. **54**, 1597 (197]).

[14] J. -H. Fock, P. Gurtler and E. E. Koch, Chem. Phys. 47,87 (1 980).

[15] L. C. Lee and J. A. Guest, J. Phys. B **14**, 3415 (1981).

[16] M. Eidelsberg, F. Launay, F. Rostas, A. Le Floch, J. Breton and B. Thieblemont, AI In, Israel. Phys. Six. 6, 240(1 984).

[17] C. Letzelter, M. Eidelsberg, F. Rostas, J. Breton and B. Thieblemont, Chem. Phys. **114**, 273 (1987).

[18] K. Yoshino, G. Stark, P. L. Smith, W. H. Parkinson and K, Ito, J. Physique **CI(3)**, CI-37 (1988).

[19] M. Eidelsberg and F. Rostas, Astron. Astrophys. 235,472 (1990).

[20] G. K. James, J. M. Ajello, 1. Kanik, B. Franklin and d. E. Shemansky, J. Phys. B 2S, 1481 (1992).

[21] P. C. Cosby, *J. Chem. Phys.* **98**, 7804 (1993).

[22] W. F. Chan, (i. Cooper and C. E. Brion, Chem. Phys. **170**, 123 (1993).

[23] A. G. Middleton, M. J. Brunger and P. J. O. Teubner, J. Phys. B **26**, 1743 (1993).

[24] I. Kanik, M. Ratliff and S. Trajmar, Chem. Phys. Lett. **208**, 341(1993).

25 D. L. Cooper and K. Kirby, J. Chem. Phys. 87,424 (1987).

26 D. E. Shemansky, J. M. Ajello, D. T. Hall, Astrophys. J. 296, 76S (1985).

27 D. E. Shemansky, J. M. Ajello, D. T. Hall and B. Franklin, Astrophys. J. 296,774 (1985).

28 J. M. Ajello, G. K. James, B. O. Franklin and D. E. Shemansky, Phys. Rev. A 40, 3524(1989).

29 G. K. James, J. M. Ajello, B. O. Franklin and D. E. Shemansky, J. Phys. B 23,2055 (1990).

30 J. M. Ajello, D. E. Shemansky, B. Franklin, J. Watkins, S. Srivastava, G. K. James, W. T. Simms, C. W. Hord, W. Pryor, W. McClintock, V. Argabright and D. Hall, Appl. Opt. 27,890 (1988).

31 H. A, Bethe, Ann. Phys. 5,325 (1930).

32 J. M. Ajello, I. Kanik, H. Bethke and D. E. Shemansky, J, Geophys. Res. (to be published, 1994).

33 D. E. Shemansky, I. Kanik, E. Bethke and J. Ajello, J. Geophys. Res. (to be published, 1994).

TABLE I

VIBRONIC EMISSION CROSS SECTIONS OF CO AT 25, 100 AND 200 eV

Feature No	Species	Wavelength (nm)	rm	Vibronic Emission Cross Section ($x10^{-18}cm^2$)		
				20eV	100eV	200eV
1	CO	107.61	$3p\pi E\ ^1\Pi(0)$-$X^1\Sigma^+$(0)	0.21	0.47	0.39
2	CO	108.79	$C^1\Sigma^+(0)$-$X^1\Sigma^+$(0	2.58	7.40	5.89
3	CO	1 5.05	$B^1\Sigma^+(0)$-$X^1\Sigma^+$(0	3.48	1.88	1.42
4	OI	115.21	^1D -$^1D^o$		0.35	0.37

TABLE II

Summary of Previous Determinations of Oscillator Strengths $f_{v'v''}$ (x 10-2) for the transitions between the different v' levels of the CO $B^1\Sigma^+$ and $C^1\Sigma^+$ states axial the ground state $X\ ^1\Sigma^+(v''=0)$

$B^1\Sigma^+$	v' = 0	v' = 1	v' = 2
Aarts and de Heera	1.5		
Lassettre and Skerbele[b]	1.53± 0.14		
Lee and Guest[c]	0.24± 0.04		
Letzelter et al.[d]	0.45	0.07	3.7×10^{-3}
Kirby and Cooper[e]	0.21	0.03	6×10^{-4}
Chan et al.[f]	0.803	0.132	
Present	1.15±0.3		

$c\ ^1\Sigma^+$	v' = 0	v = 1	v = 2	v' = 3
Aarts and de Heera	16.0			
Lassettre and Skerbele[b]	16.3 ± 1.5			
Lee and Guest[c]	1.27 ± 0.19			
Letzelter et al.[d]	6.19	0.28	$<1 \times 10^{-3}$	4.4×10^{-3}
Kirby and Cooper[e]	11.81	0.18	4×10^{-4}	1×10^{-6}
Chan et al.[f]	11.77	0.356		
Present	15.4±4.1			

[a] Ref. 12.
[b] Ref. 13.
[c] Ref. 15.
[d] Ref. 17.
[e] Theory; Ref. 2.
[f] Ref. 22.

TABLE 111

CONSTANTS OF MODIFIED BORN EQUATION(*)

CONSTANT	$B^1\Sigma^+$	$C^1\Sigma^+$
c o	0.1?786	0.0
C_1	-0.08866	0.36130
C_2	0.18946	-0,46074
C_3	-0.30905	2.62540
C4	0.0	0.0
C_5	0.23518	-1.1700
c 6	-0.23518	1.17(X)
C_7	0.058363	0.73811
C_8	0.15849	0.60256

(*) Modified Born Equation :

$$\Omega_{ij}(X) = Co \cdot (1-1/X) \cdot (X^{-2}) + \sum_{k=1}^{4} C_k \cdot (X-1) \cdot \exp(-k.C_8.X) + C_5 + C_6 / X + C_7 \cdot \ln(X)$$

FIGURE CAPTIONS

Figure 1. The intensity ratio of the (') $C\,^1\Sigma^+$ (0,0) band at 108.79 nm and the CO OII g $^4S^0$-^4P multiplet at 83.38 nm as a function of CO background gas pressure. The ratio is approximately constant up to about 2.0x 10^{-5}-Torr and starts decreasing, indicating the effect of self absorption of the CO $C\,^1\Sigma^+$ (0,0) band at 108.79 nm. The OII g $^4S^o$-^4P at 83.38 nm multiplet signal which exhibits no optical depth effects acts as a normalization feature.

Figure 2. Calibrated, nlcdium-resolution (0.025 nm FWHM) electron impact spectrum of CO at 20 eV. The spectrum was obtained in the crossed-beam mode at 1.0 x 10-5 -Torr background gas pressure. P and R branches are separated for the C - X (0,0) and B - X (0,0) transitions. Emission cross sections for the identified features arc listed in '1'able 1.

Figure 3. Calibrated, mc(fium-resolution (0.025 nm FWHM) electron impact spectrum of CO at 100 eV. The spectrum was obtained in the crossed-beam mode at 1.0 x 10^{-5}-Torr background gas pressure. P and R branches arc separated for the C - X (0,0) and B - X (0,0) transitions. Emission cross sections for the identified features are listed in Table J.

Figure 4. Calibrated, medium-resolution (0.025 nm FWHM) electron impact spectrum of CO at 200 cV. The spectrum was obtained in the crossed-beam mode at 1.0 x 10-5 -Torr background gas pressure. P and R branches arc separated for the C - X (0,0) and B - X (0,0) transitions. Emission cross sections for the identified features are listed in I'able I.

Figure S. Relative emission cross section (excitation function) of the CO $C\,^1\Sigma^+$ (0,0) band at 108.79 nm from O 10250 CV electron impact energy. Appearance Potential (Al') shown in the figure is at 11.397 eV.

Figure 6. Relative emission cross section (excitation function) of the CO $C\,^1\Sigma^+$ (0,0) band at 108.79 nm from () 101000 eV electron impact energy.

Figure 7. Relative emission cross section (excitation function) of the CO $B\,^1\Sigma^+$ (0,0) band at 115.05 nm from O to 1000 eV electron impact energy.

Figure 8. Collision strength of the CO $C\,^1\Sigma^+$ (0,0) band at 108.79 nm model and data plotted against energy (10- 1000 eV). The oscillator strength (f-value) for this feature is determined as 0.154.

Figure 9. Collision strength of the CO $B\,^1\Sigma^+$ (0.0) band at 115.05 nm model and data plotted against energy (10-1000 cV). The oscillator strength (f-value) for this feature is determined as 1.15×10^{-2}.

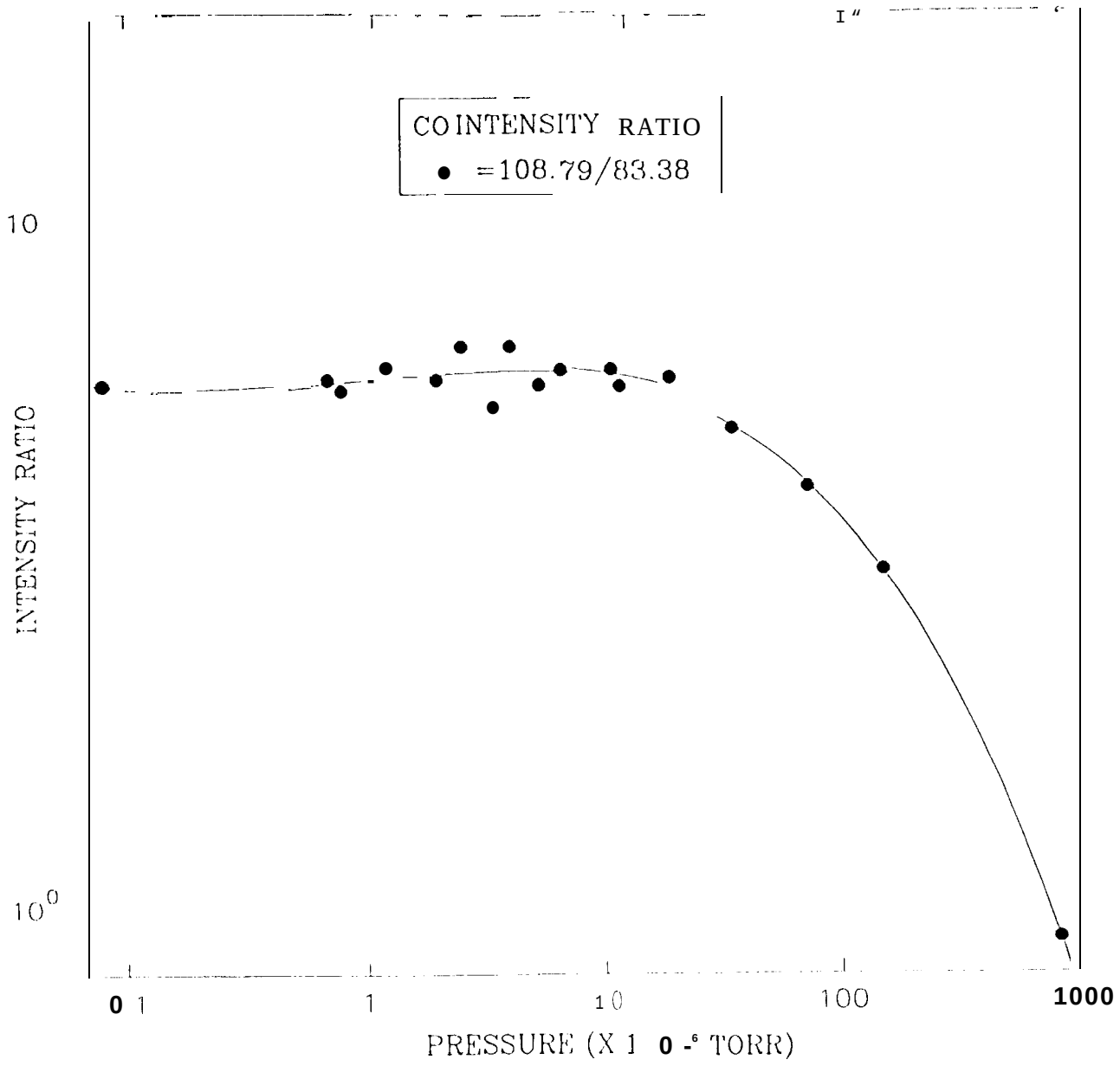
CO INTENSITY RATIO
● =108.79/83.38
10
INTENSITY RATIO
10^0
0 1
1
10
100
1000
PRESSURE (X 1 0 -6 TORR)

Fig. 1

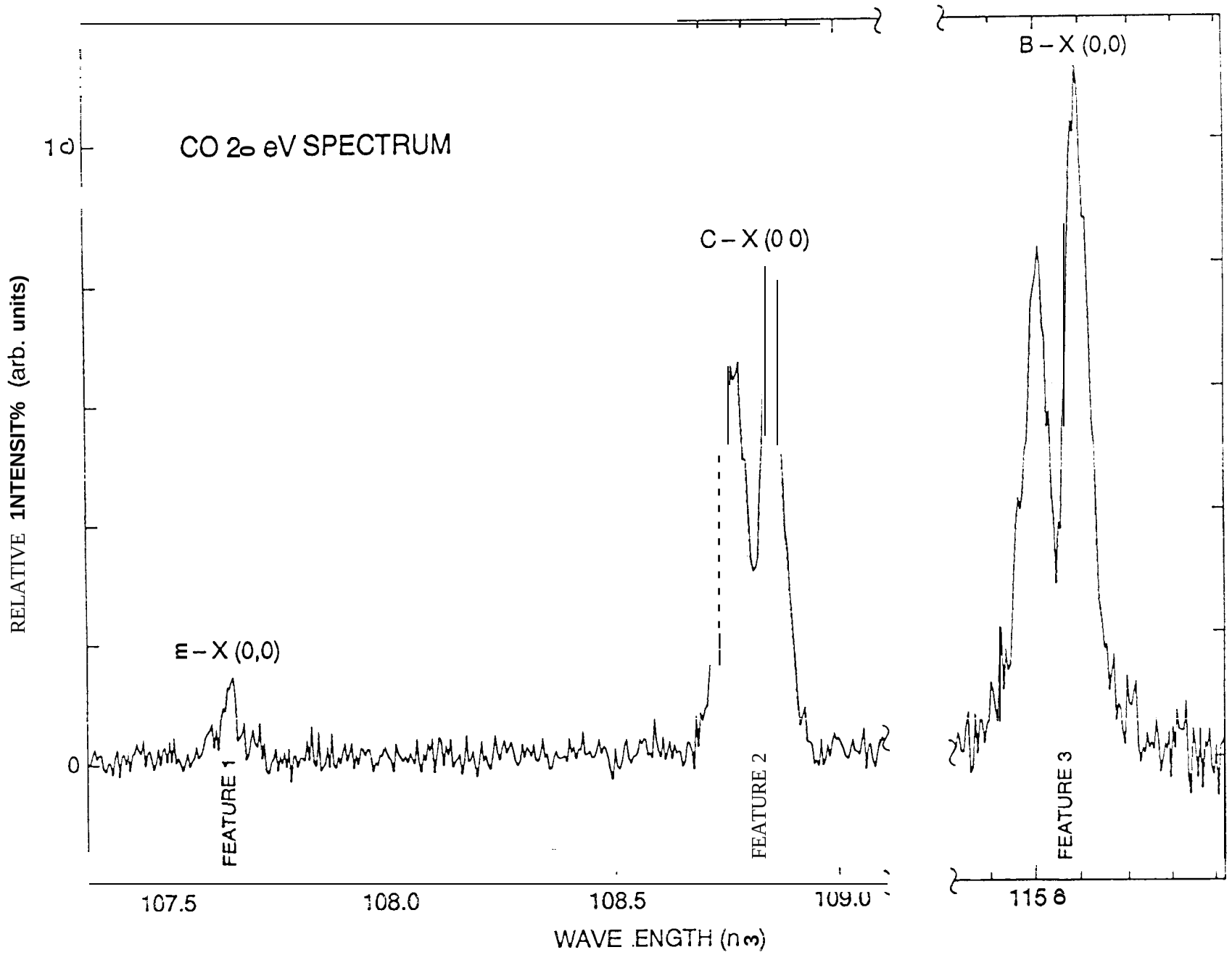
CO 2σ eV SPECTRUM
B – X (0,0)
C – X (0 0)
E – X (0,0)
FEATURE 1
FEATURE 2
FEATURE 3
RELATIVE 1NTENSIT% (arb. units)
1
0
107.5
108.0
108.5
109.0
115 6
WAVE .ENGTH (n3)

Fig. 2

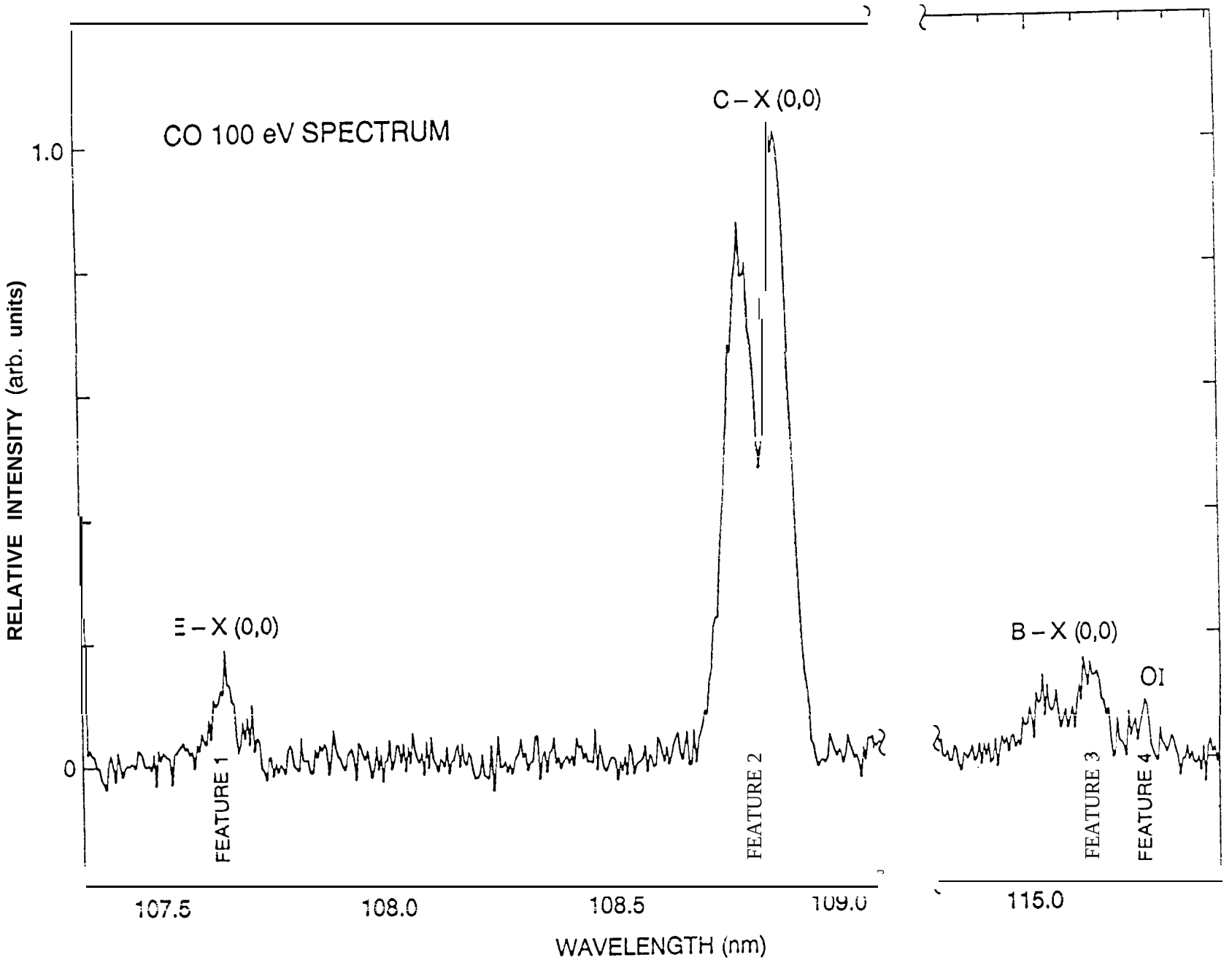
CO 100 eV SPECTRUM
C – X (0,0)
Ξ – X (0,0)
B – X (0,0)
OI
FEATURE 1
FEATURE 2
FEATURE 3
FEATURE 4
RELATIVE INTENSITY (arb. units)
1.0
0
107.5
108.0
108.5
109.0
115.0
WAVELENGTH (nm)

Fig. 3

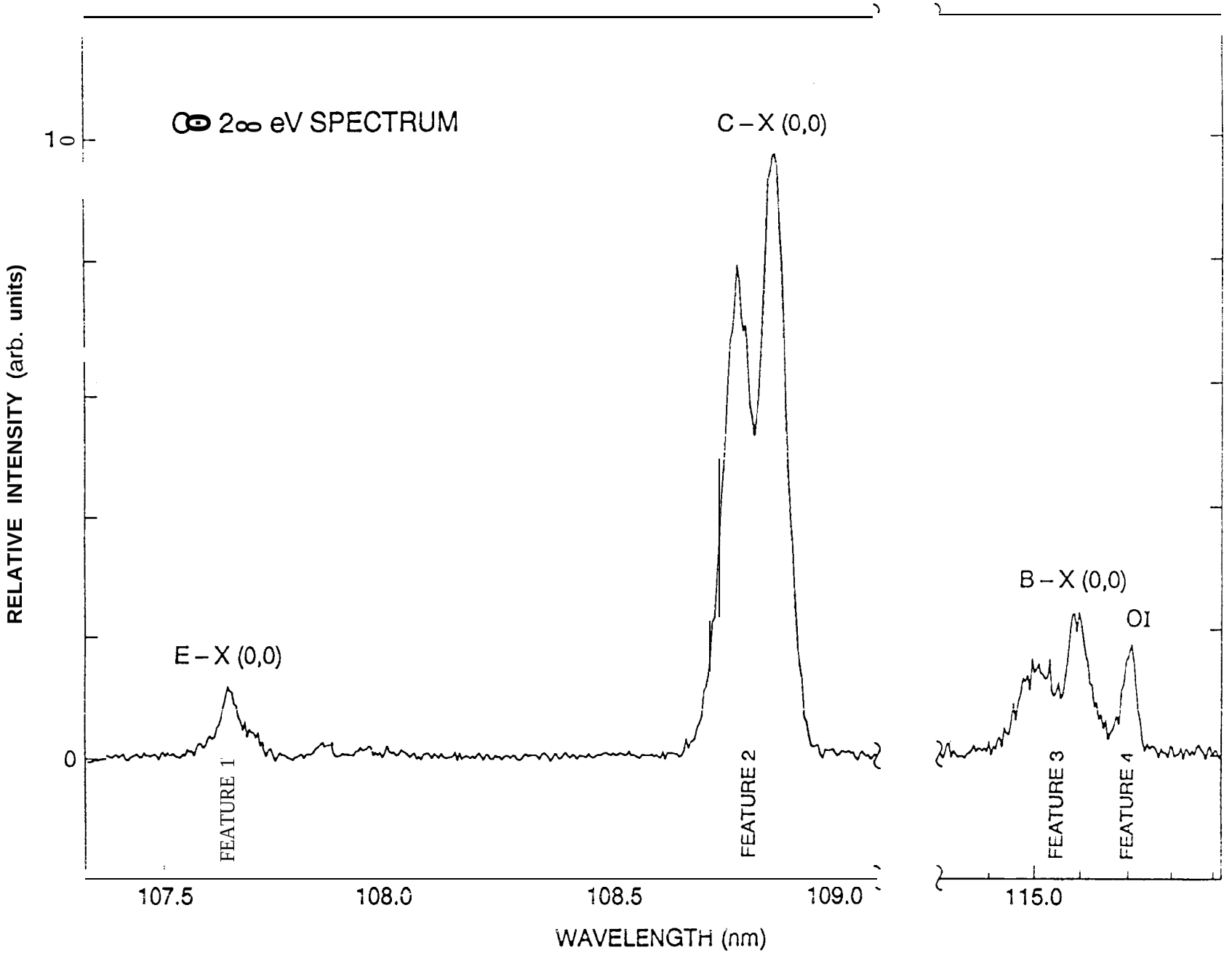
∞ 2∞ eV SPECTRUM
C – X (0,0)
E – X (0,0)
B – X (0,0)
OI
FEATURE 1
FEATURE 2
FEATURE 3
FEATURE 4
RELATIVE INTENSITY (arb. units)
1 0
0
107.5
108.0
108.5
109.0
115.0
WAVELENGTH (nm)

Fig. 4

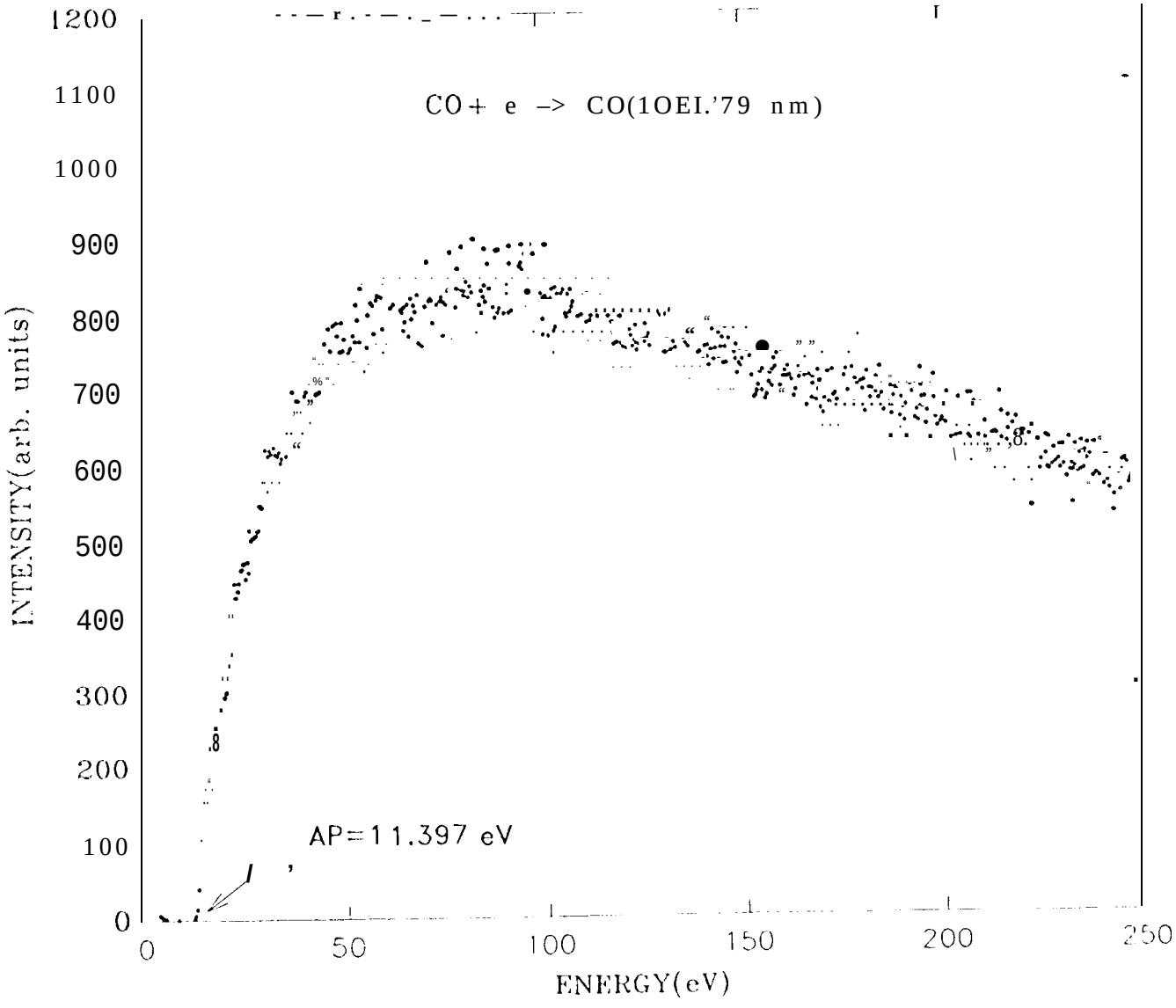
CO + e -> CO(1OEI.'79 nm)
INTENSITY(arb. units)
ENERGY(eV)
AP=11.397 eV
0
100
200
300
400
500
600
700
800
900
1000
1100
1200
0
50
100
150
200
250

Fig. 5

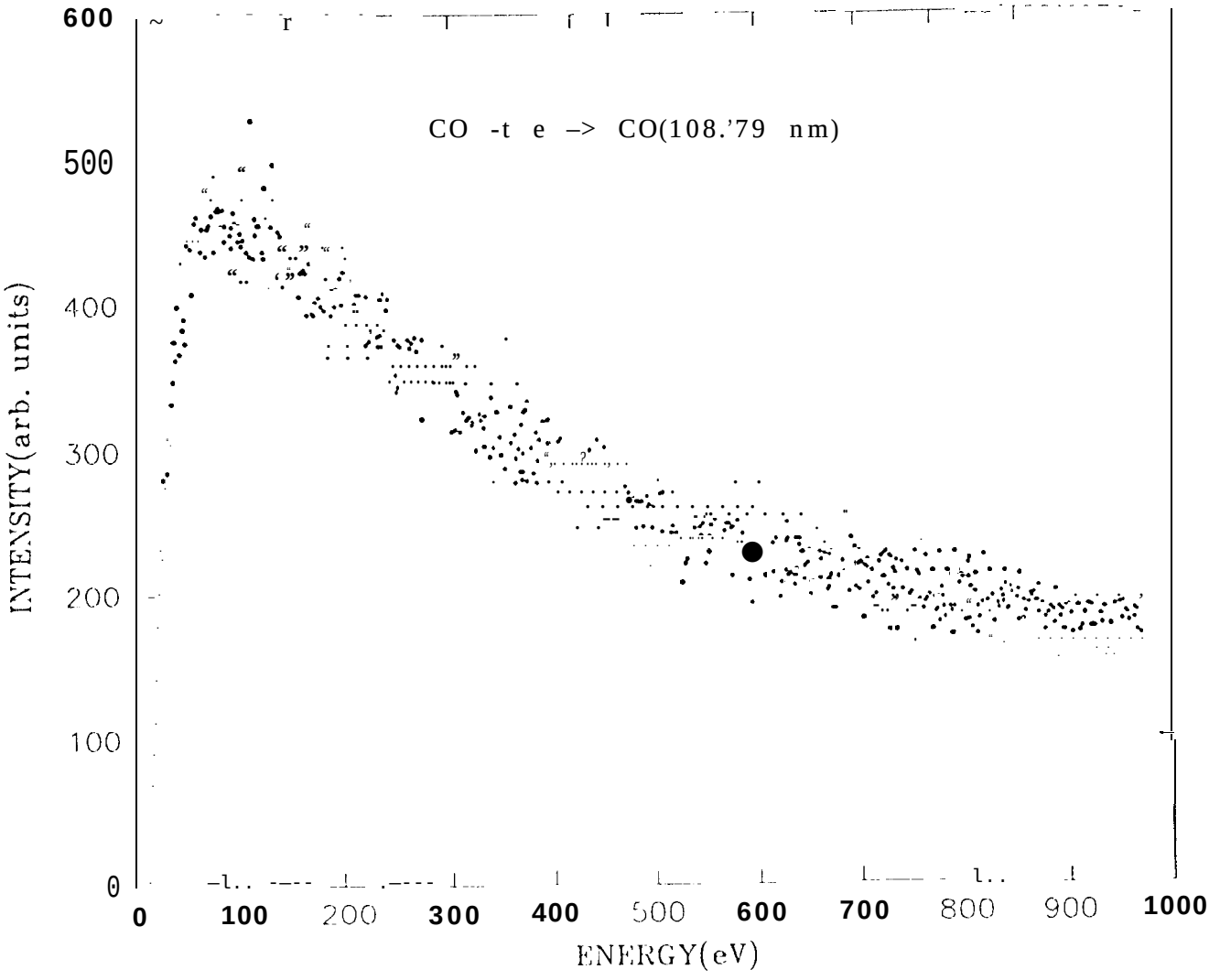
CO -t e –> CO(108.'79 nm)
INTENSITY(arb. units)
ENERGY(eV)
600
500
400
300
200
100
0
0
100
200
300
400
500
600
700
800
900
1000

Fig. 6

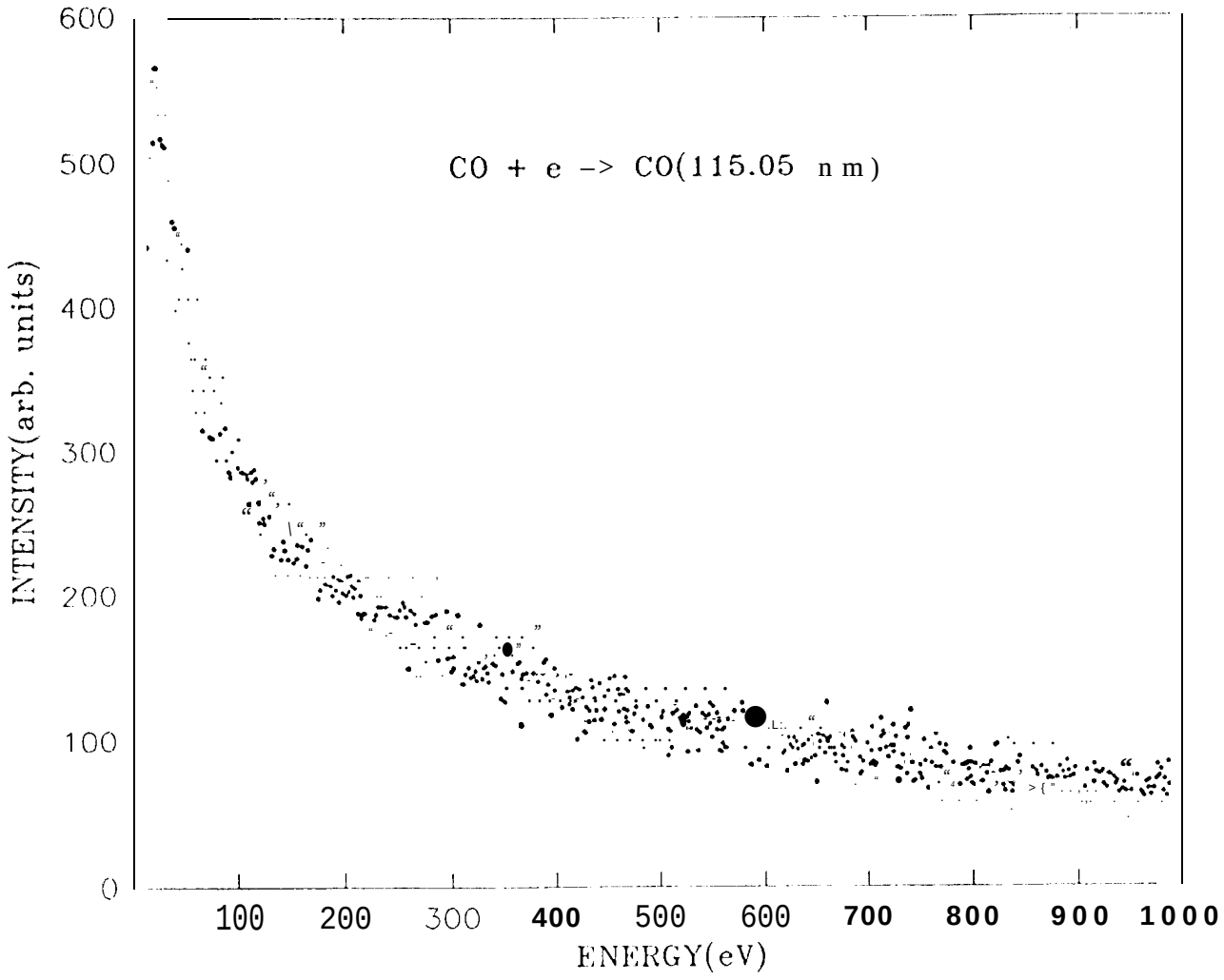
CO + e -> CO(115.05 nm)
INTENSITY(arb. units)
ENERGY(eV)
0
100
200
300
400
500
600
700
800
900
1000

Fig. 7

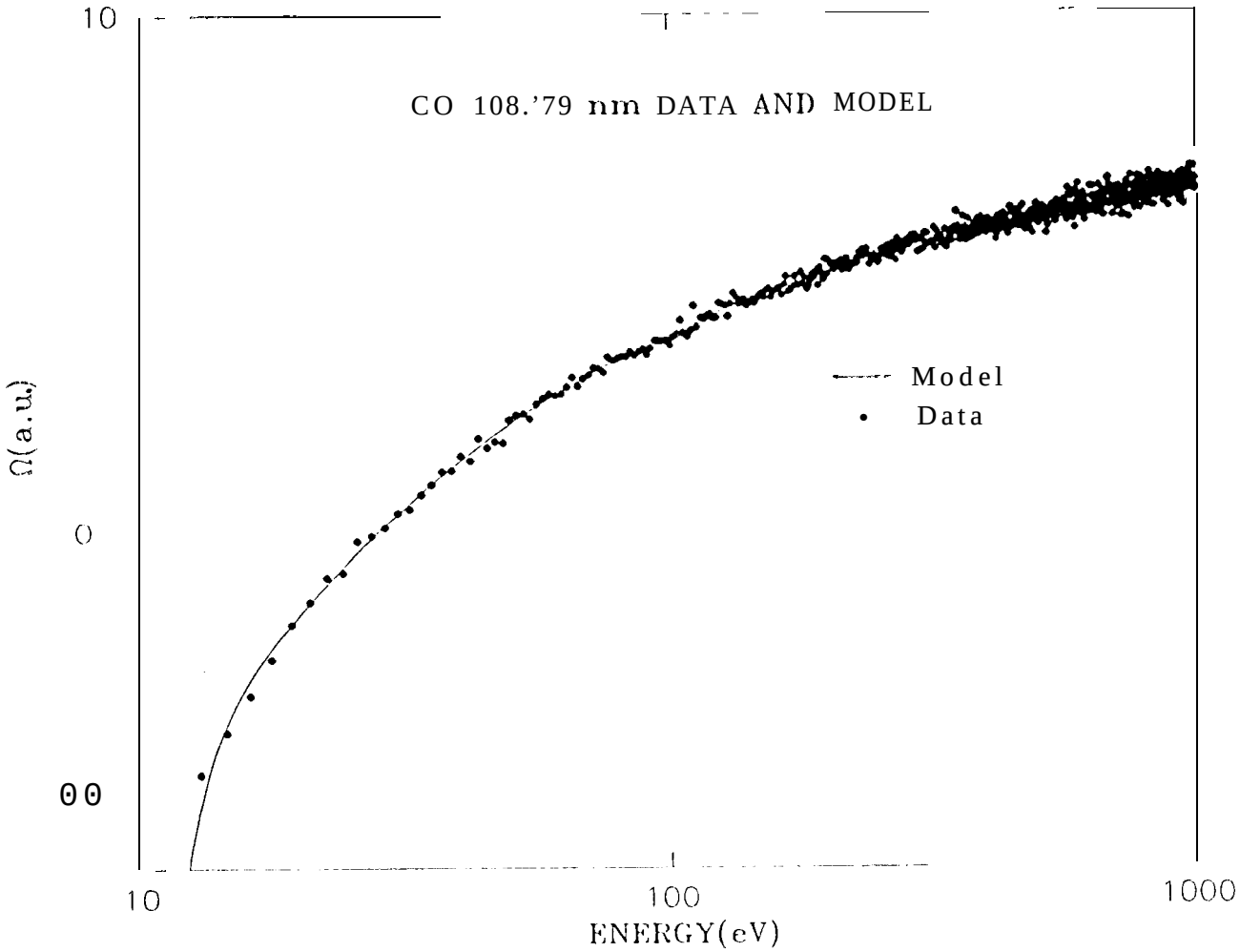
10
CO 108.'79 nm DATA AND MODEL
Model
Data
Ω(a.u.)
0
00
10
100
1000
ENERGY(eV)

Fig. 8

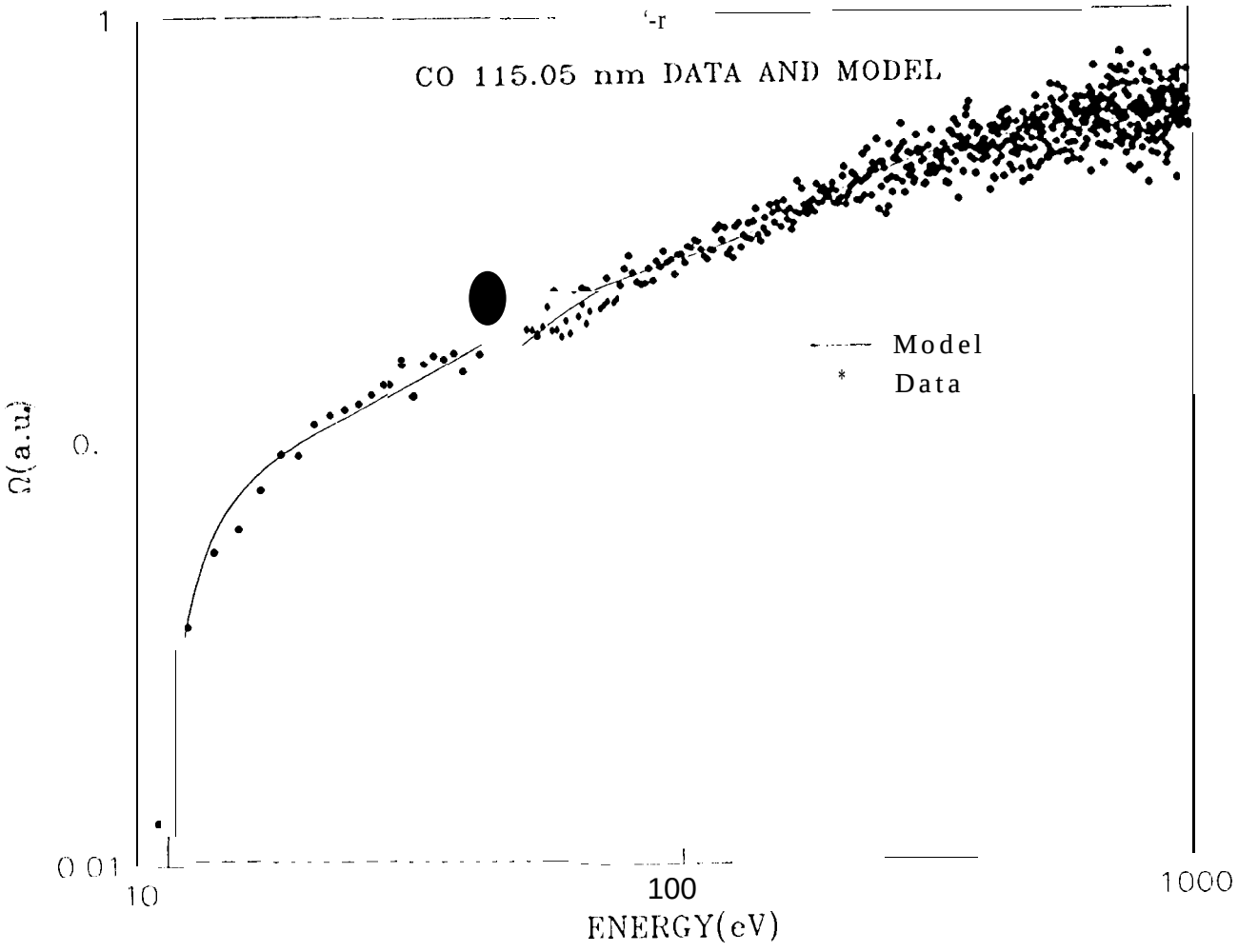
CO 115.05 nm DATA AND MODEL
Model
Data
Ω(a.u.)
1
0.
0.01
10
100
1000
ENERGY(eV)

Fig. 9